PCCP

Non-phase-separated 2D B-C-N alloys via molecule-like carbon doping in 2D BN: Atomic structures and optoelectronic properties

Journal:	*Physical Chemistry Chemical Physics*
Manuscript ID	CP-ART-05-2018-003028.R2
Article Type:	Paper
Date Submitted by the Author:	20-Aug-2018

Complete List of Authors:	Ren, Xiang-Yang; Jilin University, State Key Laboratory of Integrated Optoelectronics Xia, Sha; Jilin University, State Key Laboratory of Integrated Optoelectronics Li, Xian-Bin; JilinUniversity, State Key Laboratory of Integrated Optoelectronics; Rensselaer Polytechnic Institute, Department of Physics, Applied Physics, and Astronomy Chen, Nian-Ke; Jilin University, State Key Laboratory of Integrated Optoelectronics Wang, Xue-Peng; Jilin University, State Key Laboratory of Integrated Optoelectronics Wang, Dan; Jilin University, State Key Laboratory of Integrated Optoelectronics Chen, Zhanguo; Jilin University, State Key Laboratory of Integrated Optoelectronics Zhang, Shengbai; Rensselaer Polytechnic Institute, Department of Physics, Applied Physics, and Astronomy; Jilin University, State Key Laboratory of Integrated Optoelectronics Sun, Hongbo; Jilin University, State Key Laboratory of Integrated Optoelectronics; Tsinghua University, State Key Lab of Precision Measurement Technology and Instruments

Journal Name

ARTICLE

Non-phase-separated 2D B-C-N alloys via molecule-like carbon doping in 2D BN: Atomic structures and optoelectronic properties

Received 00th January 20xx,
Accepted 00th January 20xx

DOI: 10.1039/x0xx00000x

www.rsc.org/

Xiang-Yang Ren[a], Sha Xia[a], Xian-Bin Li[a,b*], Nian-Ke Chen[a], Xue-Peng Wang[a], Dan Wang[a], Zhan-Guo Chen[a], Shengbai Zhang[a,b], and Hong-Bo Sun[a,c]

Two-dimensional (2D) B-C-N alloys have recently attracted much attention but unfortunately, Chemical Vapor Deposition (CVD) B-C-N alloys typically phase separate. In spite of that, our analysis of the B-C-N alloy fabricated by electron-beam irradiation suggests that non-phase-separated B-C-N may in fact exist with carbon concentration up to 14 at.%. While this analysis points to a new way to overcome the phase-separation in 2D B-C-N, by first-principles calculations, we show that these B-C-N alloys are made of motifs with even-number carbon atoms, in particular, dimers or six-fold rings (in a molecule-like form), embedded in 2D BN network. Moreover, by tuning the carbon concentration, the band gap of the B-C-N alloys can be reduced by 35% from that of BN. Due to a strong overlap of the wavefunctions at the conduction band and valance band edges, the non-phase-separated B-C-N alloys maintain the strong optical absorption of BN.

Introduction

In recent years, with the development of electronic technology, the integrated density of electronic components is becoming much higher while the sizes of electronic devices are gradually decreasing. For example, the channel length of field-effect transistor (FET) is approaching its limit and is proved to be as small as 5 nm for silicon FET in 2017[1]. As a potential candidate to solve the problem, 2D semiconductors with one or several atomic thicknesses, exhibits the unique advantage in nanodevices[2-5]. Until now, a variety of 2D semiconductor materials have emerged in electronic devices, such as graphene[6-8], boron nitride[9-11], transition-metal disulfide[10, 12, 13], black phosphorus[14, 15], and so on.

As the first 2D material, graphene has drawn huge attentions since its discovery in 2004[6] due to the high carrier mobility, conductivity, high transparency, and other interesting properties[6, 16-18]. As such, it may hold applications in electrodes, transistors, flexible displays, and others[16, 19]. However, due to the shortcoming of zero band gap, it is limited to develop logic or light-emission applications. Similarly, 2D hexagonal boron nitride (*h*-BN) also has a honeycomb structure as graphene, it is a strong antioxidant which can be stable in the air up to 900 °C[20] and it has a 6.06-eV[21] or 6.07-eV[22] optical band gap. To take advantages of graphene and 2D BN, it has been proposed to combine them to be a new kind of 2D alloyed semiconductors for electronics or optoelectronics[23-26].

Up to now, both experimental and theoretical studies have made a lot of efforts to achieve 2D B-C-N alloys. For theoretical studies, in 2011 Berseneva *et al.* showed that in 2D BN the replacement of B/N with carbon is affected not only by irradiation but also by the energetics of the carbon atomic configurations[27]. In 2013, based on the first-principles calculations, Pan *et al.* found that the reaction-potential barrier of B replacing C in graphene can be reduced on the metallic ruthenium substrate[28]. Accordingly, they successfully achieved the B-doped graphene in experiment. In 2015, with the particle-swarm-optimization technique as well as the cluster-expansion method, Zhang *et al.* confirmed that the structures of 2D B-C-N systems tends to phase separate[29]. Their calculations showed that the band gaps of B-C-N systems were adjustable from that of graphene to that of BN. They also found most of the proposed candidates had direct band gaps and owned good light absorption in the visible range. For experimental studies, in 2010, Ci *et al.* successfully synthesized B-C-N systems by using methane (CH_4) and ammonia borane (NH_3-BH_3) as precursors via thermal catalytic method. However, after characterization, these composites were phase separated[30]. Nevertheless, in 2015, Wang *et al.*, on the basis of

[a] State Key Laboratory of Integrated Optoelectronics, College of Electronic Science and Engineering, Jilin University, Changchun 130012, China
[b] Department of Physics, Applied Physics, and Astronomy, Rensselaer Polytechnic Institute, Troy, New York 12180, USA
[c] State Key Lab of Precision Measurement Technology and Instruments, Department of Precision Instrument, Tsinghua University, Beijing, 100084, China
* Email: lixianbin@jlu.edu.cn

Electronic Supplementary Information (ESI) available: [details of any supplementary information available should be included here]. See DOI: 10.1039/x0xx00000x

Ci *et al*.[30], changed the synthetic precursors to trimethyl borane [$B(CH_3)_3$] and ammonia gas (NH_3). They claimed that B-C-N systems were successfully synthesized in some sense[31]. The main difference between the two experimental studies is that the former precursors contain a large number of B-N bonds, while the latter contain a large number of B-C bonds.

Although researches of B-C-N systems are still going on, the problem of phase separation is still not solved. In this work, in order to obtain the alloyed structure of 2D B-C-N without phase separation, based on the first-principles calculations and analyses on previous experiments, we dope carbon atoms into 2D BN. We find that the even-number carbon defect motifs like molecules, such as dimer and six-fold ring, manifest a lower formation energy. We construct the non-phase-separated alloys of B-C-N via doping the molecule-like carbon motifs in 2D BN with concentration from 0% to 14% (such concentrations can be found in experiment). We find that the band gaps can be modified as low as 65% of that of the BN, indicating a tuneable band gap. We also calculate the real-space charge density distribution for conduction band minimum (CBM) and valence band maximum (VBM). It is found that the CBM and VBM are both from carbon motifs as molecule-like states. The imaginary part of dielectric constant displays a good photonic absorption. The study offers an idea to overcome the difficulty of phase separation for synthesizing 2D B-C-N.

Simulation Methods

In this work, density functional theory (DFT)[32, 33] is employed as implemented in the Vienna *Ab initio* Simulation Package (VASP) codes[34]. Projector augmented wave basis[35] and Perdew-Burke-Ernzerh (PBE) functional[36] (a kind of generalized gradient approximation (GGA)[37]) are adopted. An 8 × 8 × 1 honeycomb supercell with 128 atoms is used throughout for calculations of 2D materials. All the atoms are relaxed until the Hellman-Feynman forces on individual atoms are less than 0.01 eV/Å. The cut-off energy of the plane-wave basis is 520 eV. The 1 × 1 × 1 Monkhorst-Pack k-point mesh grid are used for atomic relaxation. Spin polarization has also been considered. For comparing formation energies of other alloys, a 192-atom model of $Mo_{0.86}W_{0.14}S_2$ alloy is evaluated with cutoff energy of 360 eV and k-point mesh grid of 1 × 1 × 1.

To determine the possibility of the existence of various C defects in 2D BN, their formation energies are calculated. Usually, the formation energy $E_f(X_Y)$ of element *X* replacing element *Y* in a host material[38-41] is given as,

$$E_f(X_Y) = E_{tot}(X_Y) - E_{tot}(bulk) - \mu_{X(solid/gas)} - \mu_X^{'} + \mu_{Y(solid/gas)} + \mu_Y^{'} \quad (1)$$

where *X* is the impurity atom and *Y* is the host atom replaced by *X*. $E_{tot}(X_Y)$ is the total energy of the defective supercell (*X* replacing *Y*), and $E_{tot}(bulk)$ is the total energy of the perfect supercell without defect. $\mu_X^{'}$ and $\mu_Y^{'}$ are the chemical potentials of elements *X* and *Y* referenced to their energies in stable elementary forms (solid or gas), *i.e.* $\mu_{X(solid/gas)}$ and $\mu_{Y(solid/gas)}$. Here, $\mu_{N(N_2gas)}$, $\mu_{B(Bsolid)}$, $\mu_{C(graphene)}$ are used. All the defects are analysed in their neutral states. Since the formation of defect is determined by experimental growth conditions (such as B-rich conditions, N-rich conditions, or between them), the formation energy of defect depends on different chemical potentials. Under thermal equilibrium, the chemical potentials of host atoms must satisfy $\mu_N^{'} + \mu_B^{'} = \Delta H_f(BN)$, where $\Delta H_f(BN)$ is the formation enthalpy of the 2D BN. Under different experimental condition, $\mu_B^{'}$ and $\mu_N^{'}$ varies in the ranges as below,

(B-poor condition) $\Delta H_f(BN) \le \mu_B^{'} \le 0$ (B-rich condition) (2)

(N-poor condition) $\Delta H_f(BN) \le \mu_N^{'} \le 0$ (N-rich condition) (3)

To calculate dielectric function, we first do the geometry optimization of the constructed models and then get its ground-state electronic structure by a higher-precision static calculation. Then, we get the wavefunction from the "WAVECAR" document as an input. The parameters "LOPTICS = .TRUE." is set up to calculate the frequency dependent dielectric matrix in VASP based on the calculated single-particle electronic structure. The imaginary part is determined by a summation over the states using the equation:

$$\varepsilon_{\alpha\beta}^{(2)}(\omega) = \frac{4\pi^2 e^2}{\Omega} \lim_{q\to 0} \frac{1}{q^2} \sum_{c,v,\mathrm{K}} 2w_K \delta(\varepsilon_{cK} - \varepsilon_{vK} - \omega) \times \left\langle u_{cK} + e_{\alpha q} \middle| u_{vK} \right\rangle \left\langle u_{cK} + e_{\beta q} \middle| u_{vK} \right\rangle^* \quad (4)$$

where the indices c and v refer to conduction and valence band states, respectively. u_{cK} and u_{vK} are the cell periodic part of the orbitals at K for conduction band states and valance band states, respectively. Notice: The calculation of dielectric function requires large enough number of empty conduction band (Here, we set 776 empty bands in our 128-atom models).

Results and Discussion

In order to solve the problem of phase separation and find possible alloy structures for 2D B-C-N, we study the local C defects in 2D BN. We focus on carbon motifs with the number of atoms from 1 to 6. The structures of 35 possible candidates are shown in Fig. 1 (a). For these defects, their formation energies are calculated in the condition of $\mu_B^{'} = \mu_N^{'}$, see Fig. 1 (b). The formation energies in B rich or N rich conditions are also evaluated in Fig. S1 and Fig. S2 in supporting information (SI). Here, the notification "*m*-*n*" for the models in Fig. 1 is explained as follows: *m* represents the numbers of carbon for a defect and *n* represents the n^{th} defect. From the trend of energies in Fig. 1 (b), the carbon defects with even atom number generally have lower formation energies than those with odd atom number. Especially, we highlight three typical even-number defects in the inset of Fig.1 (b). Therefore, the carbon defects with even number should be easier to exist in BN.

In order to further illustrate the rule on defect formation, we take 6-carbon defects as examples. Fig. S3 displays their motifs. For the 6-17 and 6-18 motifs (where 2N + 4B and 2B + 4N are replaced by 6 carbons, respectively), there are two electrons less when replacing 2N + 4B and two electrons more when replacing 2B + 4N. As such, their formation energies are significantly larger due to breaking electron-number balance. In contrast, the 3N + 3B replacements (*i.e.* equal number replacement for N and B) should be more reasonable. That is because the total valance electrons of 6 carbons is just equal to those of replaced atoms. In fact, the 6-14, 6-2, 6-10, and 6-6

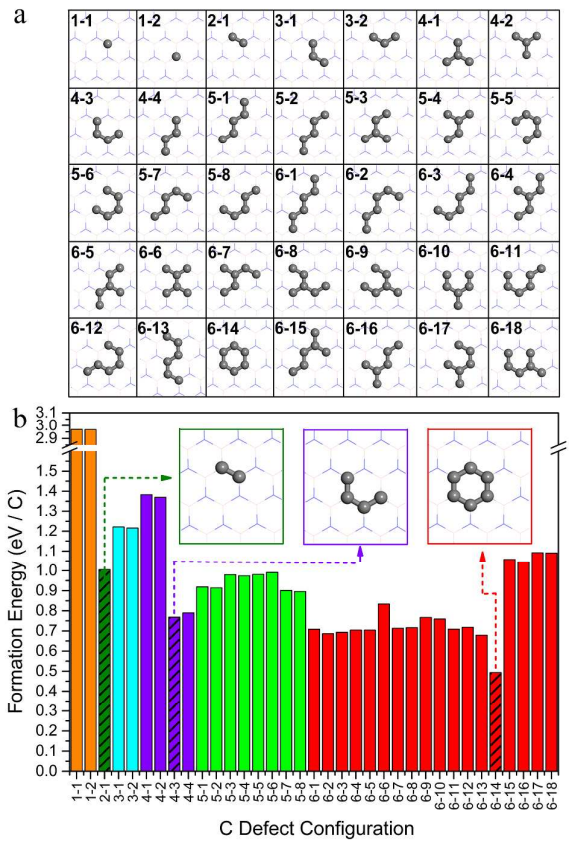

Fig. 1. (a) Possible carbon motifs doped in 2D BN. (b) Formation energy (per atom) of C defects in 2D BN in condition of $\mu_B = \mu_N$. Different colours represent the motif with different carbon number. The motifs with relatively low energy are highlighted in the insets. Color coding of atom: pink for B, blue for N, and grey for C. The notification "*m-n*" is illustrated in the main text.

defects indeed show the case. Among them, the 6-carbon honeycomb ring or say six-fold ring (6-14) holds the lowest formation energy. This is easy to be understood that the strong carbon-carbon covalent bond further stabilizes the defect. Therefore, the carbon dimer (2-1), four connected carbons inside a honeycomb ring (4-3), six-fold ring (6-14) are the most feasible defects existing in 2D BN.

In fact, an ideal 2D alloy should be the one belonging to complete solid solution systems, such as 2D $Mo_{1-x}W_xS_2$, $0<x<1$[42-44]. Here, we take 14% concentration of dopant of $Mo_{1-x}W_xS_2$ as reference, *i.e.* $Mo_{0.86}W_{0.14}S_2$, see Fig. 2(a). Fig. 2(d) indeed shows the formation energy for every W doped into MoS_2 can be as small as 0.14 eV. However, the case of a complete solid solution for $(BN)_{(1-x)/2}C_x$ is very difficult since the formation energy of every individual C doped into BN lattice [see Fig.2(c)] is as high as 2.00 eV. That explains why many previous results support a conclusion of phase separation for 2D B-C-N systems no matter from theories[29, 45, 46] or experiments[30, 31, 47-49]. However, as early as 2010, Krivanek *et al.* has carried out an interesting experiment to bombard a single BN layer by electron beam. As results, some amounts of atomic holes were opened up to facilitate the doping of C atoms as well as other elements. In their Scanning Transmission Electron Microscope (STEM) analyses, annular dark-field imaging in an aberration-corrected STEM operated

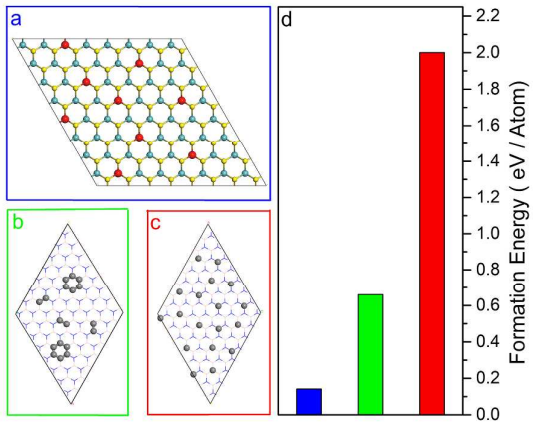

Fig. 2. Strategy to synthesize B-C-N semiconductors with lower energy. (a) W alloying MoS_2 with individual atom doping. (b) C alloying 2D BN with molecule-like doping (*i.e.* C dimer or 6-fold ring). (c) C alloying 2D BN with individual atom doping. (d) Average formation energy per dopant for the three cases above. The case for (a) is $Mo_{0.86}W_{0.14}S_2$ and the cases for (b) and (c) are $B_{0.43}N_{0.43}C_{0.14}$. In (a) the light blue, red, and yellow balls are for the Mo, W, and S atoms, respectively. Color coding for B-C-N is same as Fig. 1.

at 60 kV primary voltage can identify the positions of every atom. They showed that C atoms could be in the forms of dimer (*i.e.* the 2-1 model) and six-fold ring (*i.e.* the 6-14 model) embedded into 2D BN instead of individual atom doping[50]. In fact, some methods, for example, analyzing the electrostatic potential for atomic models is also useful to identify the atomic picture from the TEM image[51]. These observation well coincides with the present discovery of relatively low formation energy of even-number carbon defects. As such, a molecule-like carbon doping in 2D BN should be a feasible route to construct 2D B-C-N alloy. Fig. 2(b) shows one such case with 14% carbon doping. Although its formation energy (0.66 eV) is still higher than that of $Mo_{0.86}W_{0.14}S_2$, it is much lower than that of individual C doping. In fact, some special manufacturing technique could overcome the energy of molecule-like doping, such as the electron-beam-bombard facilitated doping technique, which is mentioned above[50]. In their TEM observation, as high as 14% of carbon atoms can be doped into 2D BN plane in form of dimer or six-fold ring, see the inset of the TEM picture in Fig. 3(a). Therefore, the present calculation as well as the experimental analysis offer a possible route to synthesize 2D B-C-N alloys without phase separation.

Next, we employ these two molecule-like motifs (*i.e.* carbon dimer and six-fold ring) to construct non-phase-separated B-C-N with experimentally feasible concentrations. Fig. 3(a) shows the band gaps of these B-C-N alloys decrease gradually with increasing carbon concentration. According to GGA calculations, we demonstrate the gaps can be modified from 100% to 65% of the gap of 2D BN when the dopant concentrations vary from 0% to 14%. That means a tuneable electronic property for these models. In Fig. 4 and Fig. S4 of SI, the band structures [Fig. 4 (a) and (c)] and the PDOS (partial density of states) [Fig. 4 (b) and [d]] of the typical B-C-N models are further shown. From the PDOS, we can observe that the carbon atoms mainly contribute to the VBM and CBM. But the bonding situations are slightly different between the

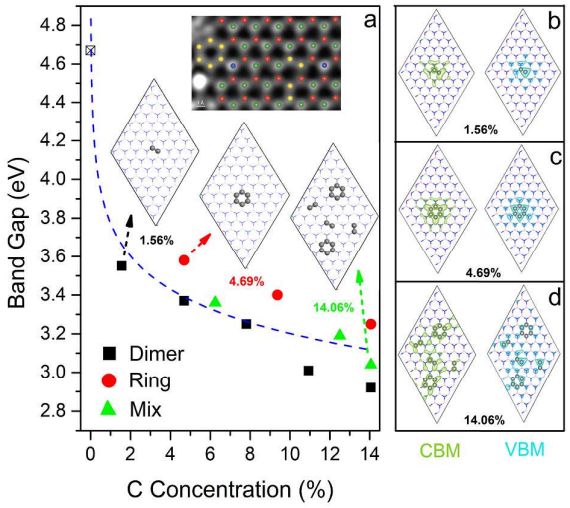

Fig. 3. Electronic properties of the proposed 2D B-C-N alloys. (a) GGA Band gap *vs.* carbon concentration. Here, black squares represent the dimer models; red circles stand for the six-fold-ring models; green triangles represent their mixing models. Distribution of CBM and VBM states in real spaces for the models with concentrations of (b) 1.56%, (c) 4.69%, and (d) 14.06%. A TEM experimental picture is reproduced with permission from ref. 50 (Copyright 2010, Nature Publishing Group) in the inset for illustration of our proposed B-C-N models without phase separation. In their TEM picture, atoms are identified as red for B, green for N, yellow for C, and blue for O.

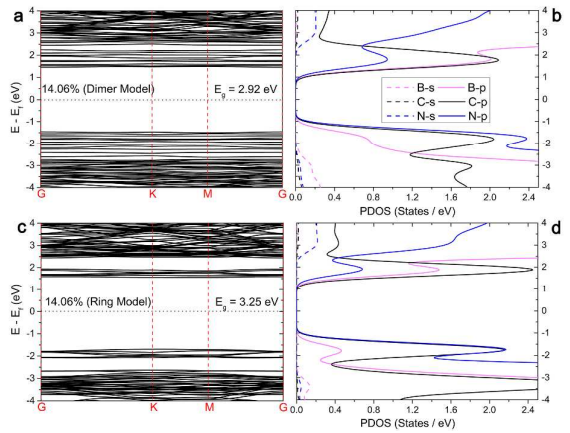

Fig. 4. Band structures and partial DOS (PDOS) of B-C-N alloy models with carbon concentration of 14.06%. (a) and (c) are the band structures for the dimer model and ring model, respectively. (b) and (d) are the PDOS of (a) and (c), respectively.

CBMs and VBMs. Their CBMs are mainly composed of carbon p orbit and boron p orbit while the VBMs are mainly composed of carbon p orbit and nitrogen p orbit. We also fit the curve of band gap *vs.* carbon concentration to see the trend. Three representative models with concentration of 1.56%, 4.69%, and 14.06% are highlighted in the inset of Fig. 3(a). Their corresponding VBM and CBM states are also plotted in the real spaces in Fig. 3(b)-(d). It is interestingly noted that the distribution of CBMs and VBMs for these B-C-N models are all around the carbon molecule-like motifs, no matter based on dimers, or six-fold rings, or their mixtures. In other words, such kind of B-C-N alloys hold molecule-like electronic states in their

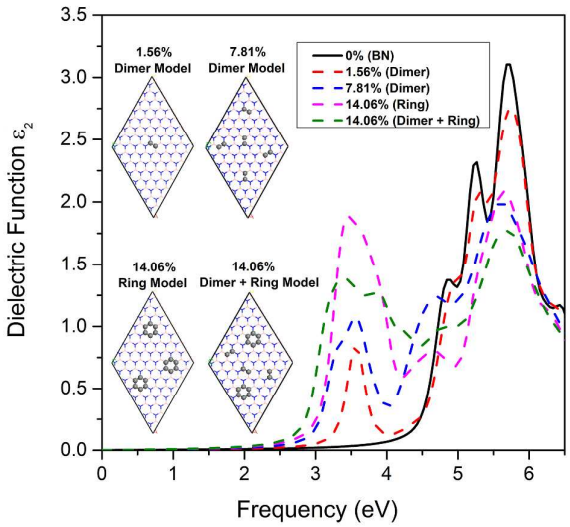

Fig. 5. In-plane dielectric function ε_2 of the proposed B-C-N models. The solid line is for the pure 2D BN and the dashed lines are for the proposed B-C-N models at their carbon concentrations up to experimentally feasible 14%.

band edge which indicate their carriers should be in form of hopping or tunneling for the transportation.

Usually, molecule-like states in semiconductors could benefit light absorptions or light emission[52]. In order to explore the application in optoelectronics, we calculate their absorption spectrum, *i.e.* imaginary part of dielectric function ε_2 for these non-phase-separated B-C-N models. Fig. 5 shows the in-plane ε_2 (*x*-axis direction, the case for the *y*-axis direction are almost the same). First of all, the molecule-like CBM and VBM together produce a strong absorption within the normal 2D BN gap, which is reflected by their strong overlap of wavefunctions to facilitate electron transition. With increasing carbon concentration, the start-up of the absorption is redshift and the intensity become stronger. This means such kinds of 2D B-C-N alloy is especially suitable for optoelectronics, such as high sensitive detector, light emitting diode (LED), and light amplification stimulated emission radiation (LASER) with designed wavelengths.

Conclusions

In sum, we find that the most likely carbon defect doped into 2D BN are the even-number molecule-like motifs, such as dimer or six-fold ring. Owning to these motifs, we construct and propose the 2D B-C-N models without phase separation. While their formation energy is still not low enough to form at the mild thermal equilibrium condition, the proposed 2D B-C-N models could be realized by certain techniques, such as electron-beam facilitated doping technique[50]. With experimentally feasible carbon concentrations (up to 14%), the proposed models have tuneable band gaps from 100% to 65% of that of 2D BN. Their CBM and VBM all locates at around carbon motifs. The strong overlap of the wavefunction of these frontier orbits make the systems especially suitable for optoelectronics. The present studies offer a feasible route to overcome the main challenge of phase separation problem for

2D B-C-N alloys fabrication. It will benefit their application on electronics.

The idea of molecule-like doping should be a useful idea to synthesize other 2D alloys which is easily phase separated. In fact, before the theoretical study (two years ago), an experimental team led by Prof. Jianlin Liu in University of California, Riverside invited us to find some possible structures for 2D B-C-N. Therefore, in the next step, we and the experimental colleagues will try to fabricate the proposed 2D B-C-N models. Furthermore, from theoretical points, the methods to get the possible n- or p-type conductivity in these B-C-N models should be also worth being explored in the near future.

Conflicts of interest

There are no conflicts to declare.

Acknowledgements

The work was supported by National Natural Science Foundation of China (No. 11874171, No. 61775077, No. 61474055), and 973 Program (No. 2014CB921303). We acknowledge the High-Performance Computing Center (HPCC) at Jilin University for calculation resources. Work at RPI was supported by the Department of Energy under Grant No. DE-SC0002623. We thank Prof. Jianlin Liu in University of California, Riverside for his helpful discussion.

References

1 N. Loubet, T. Hook, P. Montanini, C. W. Yeung, S. Kanakasabapathy, M. Guillom, T. Yamashita, J. Zhang, X. Miao and J. Wang, presented in part at the 2017 Symposium on VLSI Technology, Kyoto (Japan), 2017.
2 L. X. Zhu, F. Y. Liu, H. T. Lin, J. J. Hu, Z. F. Yu, X. R. Wang and S. H. Fan, *Light: Sci. Appl.*, 2016, **5**, e16052.
3 X. P. Wang, X. B. Li, N. K. Chen, J. H. Zhao, Q. D. Chen and H. B. Sun, *Phys. Chem. Chem. Phys.*, 2018, **20**, 6945-6950.
4 D. Wang, X. B. Li, D. Han, W. Q. Tian and H. B. Sun, *Nano Today*, 2017, **16**, 30-45.
5 X. B. Li, S. Y. Xie, H. Zheng, W. Q. Tian and H. B. Sun, *Nanoscale*, 2015, **7**, 18863-18871.
6 K. S. Novoselov, A. K. Geim, S. V. Morozov, D. Jiang, Y. Zhang, S. V. Dubonos, I. V. Grigorieva and A. A. Firsov, *Science*, 2004, **306**, 666.
7 D. Rodrigo, A. Tittl, O. Limaj, F. J. G. d. Abajo, V. Pruneri and H. Altug, *Light: Sci. Appl.*, 2017, **6**, e16277.
8 W. Strek, B. Cichy, L. Radosinski, P. Gluchowski, L. Marciniak, M. Lukaszewicz and D. Hreniak, *Light: Sci. Appl.*, 2015, **4**, e237.
9 D. Pacilé, J. C. Meyer, Ç. Ö. Girit and A. Zettl, *Appl. Phys. Lett.*, 2008, **92**, 133107.
10 M. Xu, T. Liang, M. Shi and H. Chen, *Chem. Rev.*, 2013, **113**, 3766-3798.
11 M. Autore, P. Li, I. Dolado, F. J. Alfaro-Mozaz, R. Esteban, A. Atxabal, F. Casanova, L. E. Hueso, P. Alonso-González, J. Aizpurua, A. Y. Nikitin, S. Vélez and R. Hillenbrand, *Light: Sci. Appl.*, 2018, **7**, 17172.
12 Q. H. Wang, K. Kalantarzadeh, A. Kis, J. N. Coleman and M. S. Strano, *Nat. Nanotechnol*, 2012, **7**, 699-712.
13 J. Yang, Z. Wang, F. Wang, R. J. Xu, J. Tao, S. Zhang, Q. H. Qin, B. Luther-Davies, C. Jagadish, Z. F. Yu and Y. R. Lu, *Light: Sci. Appl.*, 2016, **5**, e16046.
14 F. Xia, H. Wang and Y. Jia, *Nat. Commun.*, 2014, **5**, 4458.
15 Y. Abate, S. Gamage, Z. Li, V. Babicheva, M. H. Javani, H. Wang, S. B. Cronin and M. I. Stockman, *Light: Sci. Appl.*, 2016, **5**, e16162.
16 W. H. Lee, J. Park, S. H. Sim, S. B. Jo, K. S. Kim, B. H. Hong and K. Cho, *Adv. Mater.*, 2011, **23**, 1752-1756.
17 X. Li, Y. Zhu, W. Cai, M. Borysiak, B. Han, D. Chen, R. D. Piner, L. Colombo and R. S. Ruoff, *Nano Lett.*, 2009, **9**, 4359-4363.
18 K. S. Kim, Y. Zhao, H. Jang, S. Y. Lee, J. M. Kim, K. S. Kim, J.-H. Ahn, P. Kim, J.-Y. Choi and B. H. Hong, *Nature*, 2009, **457**, 706-710.
19 W.-H. Wang, R.-X. Du, X.-T. Guo, J. Jiang, W.-W. Zhao, Z.-H. Ni, X.-R. Wang, Y.-M. You and Z.-H. Ni, *Light: Sci. Appl.*, 2017, **6**, e17113.
20 H. Zeng, C. Zhi, Z. Zhang, X. Wei, X. Wang, W. Guo, Y. Bando and D. Golberg, *Nano Lett.*, 2010, **10**, 5049.
21 G. Kim, A. R. Jang, H. Y. Jeong, Z. Lee, D. J. Kang and H. S. Shin, *Nano Lett.*, 2013, **13**, 1834-1839.
22 L. F. Wang, B. Wu, J. S. Chen, H. T. Liu, P. A. Hu and Y. Q. Liu, *Adv. Mater.*, 2014, **26**, 1559-1564.
23 Y. Miyamoto, M. L. Cohen and S. G. Louie, *Phys. Rev. B*, 1995, **52**, 14971-14975.
24 S. Azevedo, *Eur. Phys. J. B*, 2005, **44**, 203-207.
25 O. Stephan, P. M. Ajayan, C. Colliex, P. Redlich, J. M. Lambert, P. Bernier and P. Lefin, *Science*, 1994, **266**, 1683-1685.
26 H. Pan, Y. P. Feng and J. Lin, *Phys. Rev. B*, 2006, **74**, 045409.
27 N. Berseneva, A. V. Krasheninnikov and R. M. Nieminen, *Phys. Rev. Lett.*, 2011, **107**, 035501.
28 L. Pan, Y. Que, H. Chen, D. Wang, J. Li, C. Shen, W. Xiao, S. Du, H. Gao and S. T. Pantelides, *Nano Lett.*, 2015, **15**, 6464-6468.
29 M. Zhang, G. Gao, A. Kutana, Y. Wang, X. Zou, J. S. Tse, B. I. Yakobson, H. Li, H. Liu and Y. Ma, *Nanoscale*, 2015, **7**, 12023.
30 L. Ci, L. Song, C. Jin, D. Jariwala, D. Wu, Y. Li, A. Srivastava, Z. F. Wang, K. Storr and L. Balicas, *Nat. Mater.*, 2010, **9**, 430-435.
31 H. Wang, C. Zhao, L. Liu, Z. Xu, J. Wei, W. Wang, X. Bai and E. Wang, *Nano Research*, 2016, **9**, 1221-1235.
32 P. Hohenberg and W. Kohn, *Phys. Rev.*, 1964, **136**, B864-B871.
33 W. Kohn and L. J. Sham, *Phys. Rev.*, 1965, **140**, A1133-A1138.
34 G. Kresse, Furthm, J. Uuml and ller, *Phys. Rev. B*, 1996, **54**, 11169-11186.
35 P. E. Blöchl, *Phys. Rev. B*, 1994, **50**, 17953-17979.
36 J. P. Perdew, K. Burke and M. Ernzerhof, *Phys. Rev. Lett.*, 1996, **77**, 3865-3868.
37 J. P. Perdew and W. Yue, *Phys. Rev. B*, 1986, **33**, 8800-8802.
38 S. B. Zhang and J. E. Northrup, *Phys. Rev. Lett.*, 1991, **67**, 2339.
39 D. Han, D. West, X. B. Li, S. Y. Xie, H. B. Sun and S. B. Zhang, *Phys. Rev. B*, 2010, **82**, 155132.
40 D. Wang, D. Han, X. B. Li, N. K. Chen, D. West, V. Meunier, S. B. Zhang and H. B. Sun, *Phys. Rev. B*, 2017, **96**, 155424.
41 D. Wang, D. Han, X. B. Li, S. Y. Xie, N. K. Chen, W. Q. Tian, D. West, H. B. Sun and S. B. Zhang, *Phys. Rev. Lett.*, 2015, **114**, 196801.
42 J. Y. Xi, T. Q. Zhao, D. Wang and Z. G. Shuai, *J. Phys. Chem. Lett.*, 2014, **5**, 285-291.
43 D. O. Dumcenco, H. Kobayashi, Z. Liu, Y. S. Huang and K. Suenaga, *Nat. Commun.*, 2013, **4**, 1351.
44 H. F. Liu, K. K. A. Antwi, S. Chua and D. Z. Chi, *Nanoscale*, 2014, **6**, 624-629.
45 I. Guilhon, M. Marques, L. K. Teles and F. Bechstedt, *Phys. Rev. B*, 2017, **95**, 035407.

46 K. Yuge, *Phys. Rev. B*, 2009, **79**, 144109.
47 M. O. Watanabe, S. Itoh, K. Mizushima and T. Sasaki, *Appl. Phys. Lett.*, 1996, **68**, 2962-2964.
48 M. R. Uddin, S. Majety, J. Li, J. Y. Lin and H. X. Jiang, *J. Appl. Phys.*, 2014, **115**, 093509
49 Y. Gong, G. Shi, Z. Zhang, W. Zhou, J. Jung, W. Gao, L. Ma, Y. Yang, S. Yang and Y. Ge, *Nat. Commun.*, 2014, **5**, 3193.
50 O. L. Krivanek, M. F. Chisholm, V. Nicolosi, T. J. Pennycook, G. J. Corbin, N. Dellby, M. F. Murfitt, C. S. Own, Z. S. Szilagyi, M. P. Oxley, S. T. Pantelides and S. J. Pennycook, *Nature*, 2010, **464**, 571-574.
51 S. Kurasch, J. C. Meyer, D. Kunzel, A. Gross and U. Kaiser, *Beilstein J. Nanotech.*, 2011, **2**, 394-404.
52 S. B. Zhang, S. H. Wei and A. Zunger, *Phys. Rev. B*, 2001, **63**, 075205.